PHYSICAL REVIEW B **96**, 140504(R) (2017)

Superconductivity at 5 K in quasi-one-dimensional Cr-based KCr_3As_3 single crystals

Qing-Ge Mu,[1,2] Bin-Bin Ruan,[1,2] Bo-Jin Pan,[1,2] Tong Liu,[1,2] Jia Yu,[1,2] Kang Zhao,[1,2] Gen-Fu Chen,[1,2,3] and Zhi-An Ren[1,2,3,*]

[1]*Institute of Physics and Beijing National Laboratory for Condensed Matter Physics, Chinese Academy of Sciences, Beijing 100190, China*

[2]*School of Physical Sciences, University of Chinese Academy of Sciences, Beijing 100049, China*

[3]*Collaborative Innovation Center of Quantum Matter, Beijing 100190, China*

(Received 14 August 2017; revised manuscript received 19 September 2017; published 9 October 2017)

Recently a new family of Cr-based $A_2Cr_3As_3$ (A = K, Rb, Cs) superconductors was reported, which own a rare quasi-one-dimensional (Q1D) crystal structure with infinite $(Cr_3As_3)^{2-}$ chains and exhibit intriguing superconducting characteristics possibly derived from spin-triplet electron pairing. The crystal structure of $A_2Cr_3As_3$ is actually a slight variation of the hexagonal $TlFe_3Te_3$ prototype, although they have different lattice symmetry. Here we report superconductivity in a 133-type KCr_3As_3 compound that belongs to the latter structure. The single crystals of KCr_3As_3 were prepared by the deintercalation of K ions from $K_2Cr_3As_3$ crystals which were grown from a high-temperature solution growth method, and it owns a centrosymmetric lattice in contrast to the noncentrosymmetric $K_2Cr_3As_3$. After annealing at a moderate temperature, the KCr_3As_3 crystals show superconductivity at 5 K revealed by electrical resistivity, magnetic susceptibility, and heat capacity measurements. The discovery of this KCr_3As_3 superconductor provides a different structural instance to study the exotic superconductivity in these Q1D Cr-based superconductors.

DOI: 10.1103/PhysRevB.96.140504

The recently discovered Cr-based superconductors $A_2Cr_3As_3$ (A = K, Rb, Cs) have attracted much interest besides the enthusiasm on Fe-based high-T_c superconductors [1–6]. This is partly because there have been very few Cr-containing compounds exhibiting superconductivity for a century. Except for several binary Cr alloys [7–11], the only superconductors are the lately reported ternary boride Cr_2Re_3B which has a noncentrosymmetric β-Mn-type crystal structure and a T_c of 4.8 K [12], and the binary CrAs which exhibits superconductivity at 2 K by suppressing the antiferromagnetic order via the application of external high pressures above 8 kbar [13,14]. Furthermore, these 233-type $A_2Cr_3As_3$ compounds crystallize in a very particular quasi-one-dimensional (Q1D) hexagonal crystal lattice with a space group of $P\bar{6}m2$ (No. 187), which can be regarded as infinite Q1D $(Cr_3As_3)^{2-}$ linear chains separated by alkali-metal cations that act as a charge reservoir [1–3,15]. When replacing the K^+ ions with larger Rb^+ or Cs^+ ions, the superconducting T_c decreases dramatically from 6.1 K to 4.8 and 2.2 K, respectively [1–3,15,16], and the T_c also monotonically decreases under external pressures in $K_2Cr_3As_3$ [16,17]. Theoretical calculations on $K_2Cr_3As_3$ predict a complex multiband electronic structure with a three-dimensional Fermi-surface pocket in addition to two Q1D Fermi-surface sheets mainly contributed by the Cr-3d electrons [18–22]. Experimental results show strong electron correlations and magnetic fluctuations but very diverse pictures of ground states, and both spin-triplet and spin-singlet electron pairing are proposed to explain the exotic superconductivity [23–30]. As a rare case of Q1D superconductors, $A_2Cr_3As_3$ is significantly different from previously reported Q1D superconductors such as $Li_{0.9}Mo_6O_{17}$ [31,32], $Tl_2Mo_6Se_6$ [33], and organic superconductors $(TMTSF)_2X$ (TMTSF = tetramethyltetraselenafulvalene, $X = PF_6$ or ClO_4) [34–37].

By deintercalating half of the K ions from the $K_2Cr_3As_3$ lattice, a new type of Q1D compound KCr_3As_3 can be obtained [38]. This 133-type KCr_3As_3 has a hexagonal $TlFe_3Te_3$-type crystal structure with the space group $P6_3/m$ (No. 176) [38]. Unlike its 233-type cousins which lack inversion symmetry, the KCr_3As_3 has a centrosymmetric crystal lattice. Although the characteristic Cr_3As_3 linear chain structures are similar between the two compounds except for a small-angle rotation along the c axis, removing a K^+ ion per formula from $K_2Cr_3As_3$ increases the chemical valence state of Cr and turns the Q1D chains into $(Cr_3As_3)^-$ type in the KCr_3As_3 lattice. Previous experimental studies on polycrystalline KCr_3As_3 showed cluster spin-glass ground state without superconductivity at low temperature [38], and the density functional theory first-principles calculations exhibited a magnetic Fermi surface involving only three one-dimensional sheets with much reduced dimensionality and the emergence of the interlayer antiferromagnetic order [39].

In this Rapid Communication, we report the discovery of superconductivity in the single crystals of KCr_3As_3 with a T_c of 5 K.

The 133-type KCr_3As_3 single crystals were prepared by the deintercalation of K^+ ions from $K_2Cr_3As_3$ precursors. At first, high-quality single crystals of $K_2Cr_3As_3$ were grown out of a KAs and CrAs mixture using a high-temperature solution growth method as previously reported [1]. Then the as-grown rodlike $K_2Cr_3As_3$ single crystals were immersed in pure dehydrated ethanol and kept for 1 wk for the deintercalation of K^+ ions at room temperature. The obtained samples were washed by ethanol thoroughly and labeled as sample A. To further improve the sample quality, the crystals of sample A were immersed in ethanol in a Teflon liner and loaded into an autoclave. The autoclave was tightly sealed, and sintered at 353 K for 100 h. After cooled down to room temperature, the obtained samples were washed with ethanol again and annealed in an evacuated quartz tube at 373 K for 12 h. These final postannealed KCr_3As_3 crystals were labeled as sample B. All the experimental procedures were carried out in a glovebox filled with high-purity Ar gas to avoid introducing impurities. The obtained KCr_3As_3 crystals are stable in air at room

*renzhian@iphy.ac.cn

temperature, but it decomposes above a moderate temperature at 473 K. Due to this reason, our direct synthesis of KCr_3As_3 polycrystals from solid-state reaction or single-crystal growth from high-temperature solutions all failed. For comparison, we also reproduced polycrystalline KCr_3As_3 samples by the deintercalation process from $K_2Cr_3As_3$ powders which were synthesized by a solid-state reaction method as reported [38].

The crystal structure of all samples was characterized by powder x-ray diffraction (PXRD) at room temperature with a PAN-analytical x-ray diffractometer using Cu $K\alpha$ radiation. The electrical resistivity and heat capacity were measured in a Quantum Design physical property measurement system by the standard four-probe method and relaxation method, respectively. The dc magnetization was measured in a Quantum Design magnetic property measurement system under zero-field-cooling (ZFC) and field-cooling modes.

The hexagonal crystal structure of the 133-type KCr_3As_3 is illustrated in Fig. 1(a). Due to the obvious lattice shrinkage along the a axis during the ion deintercalation process (about 8.9% from the $K_2Cr_3As_3$ precursor), the crystals of KCr_3As_3 split into threadlike filaments with micrometer-size diameters and millimeter-size lengths as shown by the scanning electron microscope image in Fig. 1(b), differing from the solid rodlike $K_2Cr_3As_3$ crystal. This crystal morphology makes it incapable for a fully single-crystal x-ray diffraction analysis for structural determination; hence PXRD is employed for structural study. Figure 1(c) shows the XRD patterns for three samples, which reveal consistent diffraction peaks with identical crystal structure. The XRD patterns of the polycrystalline sample indicate a pure single phase of the 133 structure, as indicated by the vertical bars of theoretical calculations for Bragg peak positions. The lattice parameters were refined to be $a = 9.092(1)$ Å, $c = 4.180(6)$ Å using the $P6_3/m$ (No. 176) space group, close to the previous results [38]. For the annealed single crystals of sample B, the XRD patterns on the crystal side surface only show the peaks of $(hk0)$ since the sample is threadlike along the c axis. To determine the lattice parameters, sample B was ground together with silicon powder (which acts as both an abrader and an internal standard) and the PXRD patterns show several additional diffraction peaks relevant to the c axis. We note that the KCr_3As_3 crystal has good ductility and it is difficult to make a fine powder, therefore the diffraction peaks still have a highly preferred orientation. The refined lattice parameters for sample B are $a = 9.090(8)$ Å and $c = 4.182(9)$ Å, which are very close to the results of polycrystalline samples. In addition, no obvious difference in XRD patterns for sample A and sample B was observed; and in all deintercalated samples, no diffraction peak from a possible remnant $K_2Cr_3As_3$ phase was detected. The energy-dispersive x-ray spectroscopy measurements on the crystal surface of sample B also show a 133-type ingredient with no 233 phase detected, as indicated by the "+" marks in Fig. 1(b).

The temperature dependence of electrical resistivity was characterized from 1.8 to 300 K for all samples and the data are shown in Fig. 2. In our experiments, all batches of KCr_3As_3 single crystals show superconducting transitions with resistivity dropping to zero at low temperatures. But for the polycrystalline samples, no superconductivity was observed as previously reported [38]. In Fig. 2(a), we compared the resistivity behavior between the single crystals of $K_2Cr_3As_3$ and KCr_3As_3 (both sample A and sample B). The room-temperature resistivity values are close for all these samples,

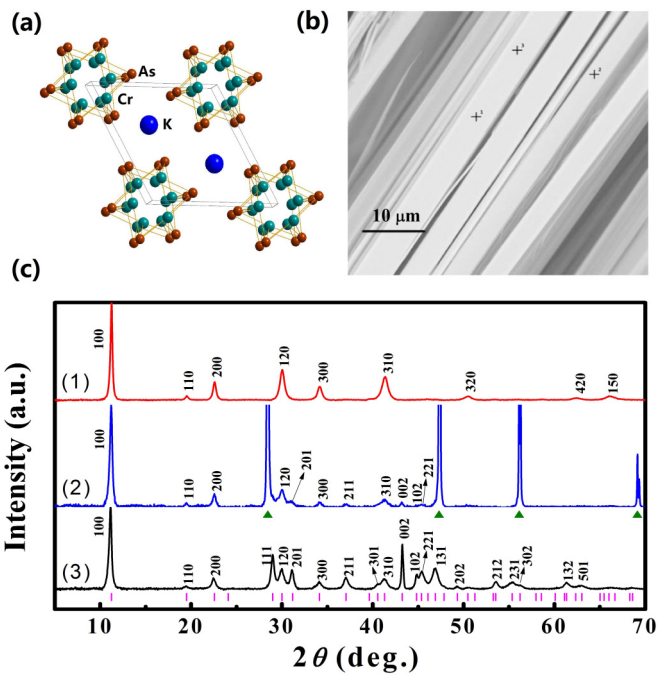

FIG. 1. (a) The hexagonal crystal structure of KCr_3As_3. (b) The scanning electron microscope image of KCr_3As_3 crystal. (c) The XRD patterns for three KCr_3As_3 samples: (1) crystals of sample B, (2) ground powder of sample B mixed with Si, and (3) polycrystalline sample. The triangles represent Bragg peaks from Si, and the vertical bars represent the position of calculated Bragg peaks.

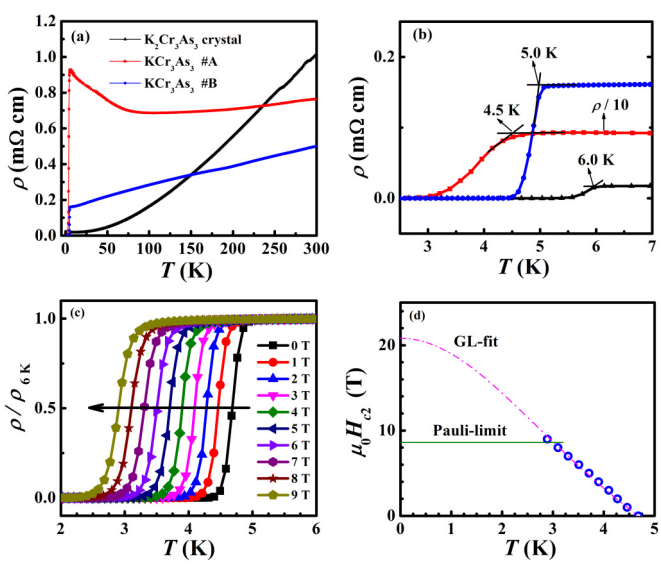

FIG. 2. (a) Temperature dependence of electrical resistivity for crystals of $K_2Cr_3As_3$ and KCr_3As_3 (both sample A and sample B). (b) Enlarged view for the resistive superconducting transitions. (c) The superconducting transitions under different magnetic fields for sample B from 0 to 9 T. (d) Derived upper critical field and the Pauli paramagnetic limit for sample B.

but the residual resistance ratio of KCr_3As_3 (∼3 for sample B) is much smaller than that of $K_2Cr_3As_3$ (∼60), indicating the poor crystalline quality of KCr_3As_3 crystals. This can be explained by the crystal defects and lattice deformation in the KCr_3As_3 crystal induced by the deintercalation process around room temperature, which also make the sample A semiconducting-like behavior below 100 K, while after annealing, the crystal quality becomes better and it shows a metallic resistivity behavior for sample B. This can be further illustrated by the superconducting transition as shown in Fig. 2(b). Sample A shows a wide superconducting transition and an onset $T_c \sim 4.5$ K, while sample B shows a much narrower superconducting transition with a higher onset $T_c \sim 5.0$ K, and both values are lower than the $T_c \sim 6.0$ K of $K_2Cr_3As_3$.

To further characterize the superconducting properties, we performed resistivity measurements on sample B under constant magnetic fields from 0 to 9 T with sweeping temperature to study the upper critical field H_{c2} (with the field perpendicular to the c axis and electrical current along the c axis), and the normalized data for $\rho/\rho_{6\,\mathrm{K}}$ vs T are shown in Fig. 2(c). With magnetic field increasing, the T_c shifts to lower temperatures systematically. We define the $\mu_0 H_{c2}$ as the field determined by 50% of the normal-state resistivity at T_c, and it was depicted as a function of temperature in Fig. 2(d). Considering the Ginzburg-Landau theory, $\mu_0 H_{c2}(T) = \mu_0 H_{c2}(0)(1-t^2)/(1+t^2)$, here $t = T/T_c$, the zero-temperature upper critical field $\mu_0 H_{c2}(0)$ is estimated to be 20.8 T. This value is much higher than the Pauli paramagnetic limited upper critical field $\mu_0 H_p = 1.84 T_c \approx 8.6$ T [40], which gives evidence for unconventional superconductivity in KCr_3As_3, and a similar phenomenon was also reported in $Li_{0.9}Mo_6O_{17}$ [41], Sr_2RuO_4 [42], and $K_2Cr_3As_3$ superconductors [1].

To demonstrate whether the observed superconductivity is the bulk nature of the K-133 phase or from a possible minor remnant K-233 phase which cannot be detected by XRD, the temperature dependence of magnetic susceptibility and heat capacity were characterized and shown in Fig. 3. Under a magnetic field of 10 Oe (perpendicular to the c axis), samples A and B show a clear diamagnetic superconducting transition at 3.7 and 4.7 K, respectively. Whereas, the shielding volume fraction at 2 K from the ZFC data is only about 9% for sample A, and it is significantly enhanced to nearly 98% for sample B. This is consistent with the behavior of a resistive superconducting transition. The results indicate that sample A only shows very poor superconductivity with a small superconducting fraction, while after annealing, as the crystal lattice is reformed, sample B becomes a good superconductor. For the normal-state susceptibility of sample B, it roughly coincides with the Curie-Weiss behavior with no magnetic ordering transition. In Fig. 3(c) we show the isothermal magnetization curve of sample B with respect to a magnetic field from −5 to 5 T at 2 K, and it reveals typical type-II superconductivity in single-crystalline KCr_3As_3.

The temperature dependence of heat capacity is plotted in Fig. 3(d) as a relationship for C_p/T vs T^2. The normal-state data are linearly fitted with both electron and phonon contributions by $C_p/T = \gamma + \beta T^2$ with T above T_c, from which we obtain the Sommerfeld coefficient γ as 81.31 mJ/(mol K^2), and Debye temperature θ_D as 319 K calculated according to $\theta_D = [(12/5)\mathrm{NR}\pi^4/\beta]^{1/3}$. Comparing with $K_2Cr_3As_3$, the close γ values indicate similar strong electron correlations, while the higher θ_D is reasonably originated from the condensed crystal lattice for KCr_3As_3 [1,16]. The clear heat capacity jump in the C_p curve happens at about 5 K. This indicates the occurrence of a superconducting transition and further confirms the superconductivity of KCr_3As_3 single crystals, which is consistent with the results of resistivity and magnetization measurements. We note that the value of the heat capacity jump $\Delta C_p/\gamma T_c$ is about 0.47, which is much smaller than that of $K_2Cr_3As_3$ [1]; this is probably due to the low sample quality by remaining crystal defects which are not fully removed during the annealing process with the relatively low annealing temperature of only 373 K. To further exclude the possibility of a remnant K-233 superconducting phase inside the crystals, the powders of mashed K-133 single crystals were exposed in air for several days and no clear change was observed for the superconducting diamagnetism. This is distinctly different from the K-233 powders which are extremely reactive and burn immediately when exposed in air. The similar superconducting and electronic characteristics in KCr_3As_3 and $K_2Cr_3As_3$ possibly indicate same electron pairing mechanism that derives from a different lattice symmetry, and the lack of superconductivity in polycrystalline KCr_3As_3 and the annealing effects for single crystals reveal the extreme sensitivity of superconductivity by disorders in the crystal lattice.

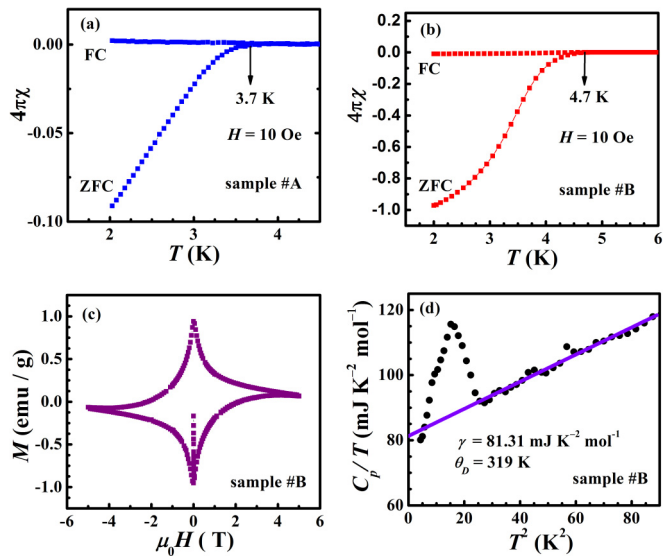

FIG. 3. Temperature dependence of magnetic susceptibility for (a) sample A and (b) sample B. (c) Isothermal magnetization for sample B at 2 K. (d) Low-temperature heat capacity for sample B depicted as C_p/T vs T^2 with a normal state linear fit.

In summary, we synthesized the 133-type KCr_3As_3 single crystals, and found superconductivity at a T_c of 5.0 K. This compound has a centrosymmetric crystal structure differing from its noncentrosymmetric counterpart $K_2Cr_3As_3$. Considering similar superconducting characteristics but different crystal symmetry between the two superconductors, this KCr_3As_3 provides another platform to acquire deep insight into the unconventional superconducting mechanism in these Q1D Cr-based superconductors.

The authors are grateful for the financial support from the National Natural Science Foundation of China (Grant No. 25311474339), the National Basic Research Program of China (973 Program, Grant No. 2016YFA0300301), and the Youth Innovation Promotion Association of the Chinese Academy of Sciences.

[1] J. K. Bao, J. Y. Liu, C. W. Ma, Z. H. Meng, Z. T. Tang, Y. L. Sun, H. F. Zhai, H. Jiang, H. Bai, C. M. Feng, Z. A. Xu, and G. H. Cao, Phys. Rev. X **5**, 011013 (2015).
[2] Z. T. Tang, J. K. Bao, Y. Liu, Y. L. Sun, A. Ablimit, H. F. Zhai, H. Jiang, C. M. Feng, Z. A. Xu, and G. H. Cao, Phys. Rev. B **91**, 020506 (2015).
[3] Z. T. Tang, J. K. Bao, Z. Wang, H. Bai, H. Jiang, Y. Liu, H. F. Zhai, C. M. Feng, Z. A. Xu, and G. H. Cao, Sci. China Mater. **58**, 16 (2015).
[4] Y. Kamihara, T. Watanabe, M. Hirano, and H. Hosono, J. Am. Chem. Soc. **130**, 3296 (2008).
[5] Z. A. Ren, W. Lu, J. Yang, W. Yi, X. L. Shen, C. Zheng, G. C. Che, X. L. Dong, L. L. Sun, F. Zhou, and Z. X. Zhao, Chin. Phys. Lett. **25**, 2215 (2008).
[6] Y. Kamihara, H. Hiramatsu, M. Hirano, R. Kawamura, H. Yanagi, T. Kamiya, and H. Hosono, J. Am. Chem. Soc. **128**, 10012 (2006).
[7] K. Andres, E. Bucher, J. P. Maita, and R. C. Sherwood, Phys. Rev. **178**, 702 (1969).
[8] E. Bucher, F. Heiniger, J. Muheim, and J. Muller, Rev. Mod. Phys. **36**, 146 (1964).
[9] B. Matthias, V. B. Compton, H. Suhl, and E. Corenzwit, Phys. Rev. **115**, 1597 (1959).
[10] B. T. Matthias, T. H. Geballe, V. B. Compton, E. Corenzwit, and G. W. Hull, Phys. Rev. **128**, 588 (1962).
[11] T. F. Smith, J. Low Temp. Phys. **6**, 171 (1972).
[12] H. Niimura, K. Kawashima, K. Inoue, M. Yoshikawa, and J. Akimitsu, J. Phys. Soc. Jpn. **83**, 044702 (2014).
[13] H. Kotegawa, S. Nakahara, H. Tou, and H. Sugawara, J. Phys. Soc. Jpn. **83**, 093702 (2014).
[14] W. Wu, J. Cheng, K. Matsubayashi, P. Kong, F. Lin, C. Jin, N. Wang, Y. Uwatoko, and J. Luo, Nat. Commun. **5**, 5508 (2014).
[15] X. F. Wang, C. Roncaioli, C. Eckberg, H. Kim, J. Yong, Y. Nakajima, S. R. Saha, P. Y. Zavalij, and J. Paglione, Phys. Rev. B **92**, 020508 (2015).
[16] T. Kong, S. L. Bud'ko, and P. C. Canfield, Phys. Rev. B **91**, 020507 (2015).
[17] Z. Wang, W. Yi, Q. Wu, V. A. Sidorov, J. K. Bao, Z. T. Tang, J. Guo, Y. Z. Zhou, S. Zhang, H. Li, Y. G. Shi, X. X. Wu, L. Zhang, K. Yang, A. G. Li, G. H. Cao, J. P. Hu, L. L. Sun, and Z. X. Zhao, Sci. Rep. **6**, 37878 (2016).
[18] H. Jiang, G. H. Cao, and C. Cao, Sci. Rep. **5**, 16054 (2015).
[19] X. X. Wu, F. Yang, C. C. Le, H. Fan, and J. P. Hu, Phys. Rev. B **92**, 104511 (2015).
[20] X. X. Wu, C. C. Le, J. Yuan, H. Fan, and J. P. Hu, Chin. Phys. Lett. **32**, 057401 (2015).
[21] L. D. Zhang, X. X. Wu, H. Fan, F. Yang, and J. P. Hu, Europhys. Lett. **113**, 37003 (2016).
[22] H. T. Zhong, X. Y. Feng, H. Chen, and J. H. Dai, Phys. Rev. Lett. **115**, 227001 (2015).
[23] D. T. Adroja, A. Bhattacharyya, M. Telling, Y. Feng, M. Smidman, B. Pan, J. Zhao, A. D. Hillier, F. L. Pratt, and A. M. Strydom, Phys. Rev. B **92**, 134505 (2015).
[24] G. M. Pang, M. Smidman, W. B. Jiang, J. K. Bao, Z. F. Weng, Y. F. Wang, L. Jiao, J. L. Zhang, G. H. Cao, and H. Q. Yuan, Phys. Rev. B **91**, 220502 (2015).
[25] G. M. Pang, M. Smidman, W. B. Jiang, Y. G. Shi, J. K. Bao, Z. T. Tang, Z. F. Weng, Y. F. Wang, L. Jiao, J. L. Zhang, J. L. Luo, G. H. Cao, and H. Q. Yuan, J. Magn. Magn. Mater. **400**, 84 (2016).
[26] J. Yang, Z. T. Tang, G. H. Cao, and G. Q. Zheng, Phys. Rev. Lett. **115**, 147002 (2015).
[27] W. L. Zhang, H. Li, D. Xia, H. W. Liu, Y. G. Shi, J. L. Luo, J. Hu, P. Richard, and H. Ding, Phys. Rev. B **92**, 060502 (2015).
[28] H. Z. Zhi, D. Lee, T. Imai, Z. T. Tang, Y. Liu, and G. H. Cao, Phys. Rev. B **93**, 174508 (2016).
[29] H. Z. Zhi, T. Imai, F. L. Ning, J. K. Bao, and G. H. Cao, Phys. Rev. Lett. **114**, 147004 (2015).
[30] F. F. Balakirev, T. Kong, M. Jaime, R. D. McDonald, C. H. Mielke, A. Gurevich, P. C. Canfield, and S. L. Bud'ko, Phys. Rev. B **91**, 220505 (2015).
[31] M. Greenblatt, W. H. McCarroll, R. Neifeld, M. Croft, and J. V. Waszczak, Solid State Commun. **51**, 671 (1984).
[32] M. H. Whangbo and E. Canadell, J. Am. Chem. Soc. **110**, 358 (1988).
[33] J. C. Armici, M. Decroux, Ø. Fischer, M. Potel, R. Chevrel, and M. Sergent, Solid State Commun. **33**, 607 (1980).
[34] D. Jérome, A. Mazaud, M. Ribault, and K. Bechgaard, J. Phys. Lett. **41**, 95 (1980).
[35] K. Bechgaard, K. Carneiro, M. Olsen, F. B. Rasmussen, and C. S. Jacobsen, Phys. Rev. Lett. **46**, 852 (1981).
[36] K. Bechgaard, K. Carneiro, F. B. Rasmussen, M. Olsen, G. Rindorf, C. S. Jacobsen, H. J. Pedersen, and J. C. Scott, J. Am. Chem. Soc. **103**, 2440 (1981).
[37] F. Wudl, J. Am. Chem. Soc. **103**, 7064 (1981).
[38] J. K. Bao, L. Li, Z. T. Tang, Y. Liu, Y. K. Li, H. Bai, C. M. Feng, Z. A. Xu, and G. H. Cao, Phys. Rev. B **91**, 180404 (2015).
[39] C. Cao, H. Jiang, X. Y. Feng, and J. Dai, Phys. Rev. B **92**, 235107 (2015).
[40] A. M. Clogston, Phys. Rev. Lett. **9**, 266 (1962).
[41] J. F. Mercure, A. F. Bangura, X. F. Xu, N. Wakeham, A. Carrington, P. Walmsley, M. Greenblatt, and N. E. Hussey, Phys. Rev. Lett. **108**, 187003 (2012).
[42] K. D. Nelson, Z. Q. Mao, Y. Maeno, and Y. Liu, Science **306**, 1151 (2004).